As per UGC guidelines an electronic bar code is provided to secure your paper

International Journal for Modern Trends in Science and Technology
Volume 12, Issue 07, pages 139-149.
ISSN: 2455-3778 online
Available online at: http://www.ijmtst.com/vol12issue06.html
DOI: https://doi.org/10.5281/zenodo.20739616

ANN-Based Renewable Energy Integrated Bidirectional EV Charging System Using Solar PV, BESS, and Dual Active Bridge Converter

Syeda Shagufta [1] | A. Rajesh[2] | Dr. K. Siva Kumar[3]

[1]*PG Student, Dept. of Electrical & Electronics Engineering, Sri Venkatesa Perumal College of Engineering and Technology, Puttur, Andhra Pradesh, India*
[2]*Assistant Professor, Dept. of Electrical & Electronics Engineering, Sri Venkatesa Perumal College of Engineering and Technology, Puttur, Andhra Pradesh, India*
[3]*Professor, Dept. of Electrical & Electronics Engineering, Sri Venkatesa Perumal College of Engineering and Technology, Puttur, Andhra Pradesh, India*

To Cite this Article
Syeda Shagufta, A. Rajesh & Dr. K. Siva Kumar (2026). ANN-Based Renewable Energy Integrated Bidirectional EV Charging System Using Solar PV, BESS, and Dual Active Bridge Converter. International Journal for Modern Trends in Science and Technology, 12(07), 139-149. https://doi.org/10.5281/zenodo.20739616

Article Info
Received: 05 June 2026; Revised: 05 July 2026; Accepted: 08 July 2026.

KEYWORDS

Electric Vehicle (EV), Solar Photovoltaic (PV), Maximum Power Point Tracking, Battery Energy Storage System, Bidirectional Buck–Boost Converter, Dual Active Bridge (DAB), Artificial Neural Network, Phase-Shifted PWM (PSPWM), Bidirectional EV Charging.

ABSTRACT

The increasing penetration of electric vehicles (EVs) and renewable energy resources has accelerated the need for intelligent and efficient charging systems. This paper presents an ANN-based renewable energy integrated bidirectional EV charging system consisting of a Solar Photovoltaic (PV) source, Battery Energy Storage System (BESS), DC–DC boost converter, bidirectional buck–boost converter, and an isolated Dual Active Bridge (DAB) converter. The Solar PV system employs a Perturb and Observe (P&O) Maximum Power Point Tracking (MPPT) algorithm to maximize power extraction under varying irradiance conditions, while the boost converter regulates the PV output voltage. The BESS is interfaced through a bidirectional buck–boost converter with a voltage and current control scheme to regulate the DC-link voltage and manage battery charging and discharging operations. An ANN-based current controller combined with Phase-Shifted Pulse Width Modulation (PSPWM) controls the DAB converter to achieve accurate charging current regulation and efficient bidirectional power transfer to the EV battery. The proposed system is modeled and simulated in MATLAB/Simulink. Simulation results demonstrate stable DC-link voltage, effective power sharing between the Solar PV source and BESS, reduced current ripple, enhanced EV battery state of charge (SOC), and improved overall charging efficiency. The proposed system provides an intelligent, reliable, and energy-efficient solution for next-generation renewable energy-powered bidirectional EV charging applications.

1. INTRODUCTION

The rapid advancement of electric vehicles (EVs) has significantly accelerated the transition toward sustainable transportation by reducing greenhouse gas emissions and dependence on conventional fossil fuels. However, the increasing penetration of EVs has introduced new challenges to modern power systems, including increased electricity demand, peak load variations, voltage fluctuations, and power quality issues. To address these challenges, renewable energy-powered EV charging stations integrated with intelligent energy management systems have become an attractive solution for future smart grids [1], [2]. Among the available renewable energy sources, Solar Photovoltaic (PV) technology has received considerable attention because of its clean energy production, low maintenance requirements, and widespread availability [3]. Nevertheless, the output power of PV systems is highly dependent on solar irradiance and ambient temperature, resulting in continuous power fluctuations [4]. Therefore, Maximum Power Point Tracking (MPPT) techniques are essential for extracting the maximum available power from PV arrays. Among various MPPT algorithms, the Perturb and Observe (P&O) method is widely adopted because of its simple implementation, fast convergence, and satisfactory performance under varying environmental conditions [5], [6]. In the proposed system, the Solar PV array is connected to the DC-link through a DC–DC boost converter controlled by the P&O MPPT algorithm to maximize renewable energy utilization and maintain a regulated DC-link voltage. To improve the reliability of renewable energy-powered EV charging stations, a Battery Energy Storage System (BESS) is integrated into the charging architecture. The BESS stores excess solar energy during periods of high PV generation and supplies power when solar generation is insufficient or EV charging demand increases [7]. This coordinated operation improves energy utilization, enhances charging continuity, and reduces dependence on the utility grid [8]. The battery is interfaced with the common DC-link using a bidirectional buck–boost converter, which enables both charging and discharging operations while maintaining stable battery voltage and current through dedicated control loops [9]. The voltage and current controllers ensure effective battery energy management, improve converter stability, and extend battery lifetime [10]. Efficient bidirectional power conversion is another important requirement for modern EV charging systems. Conventional isolated DC–DC converters generally suffer from increased switching losses and reduced efficiency at high power levels [11]. The Dual Active Bridge (DAB) converter has emerged as one of the most suitable converter topologies because it provides galvanic isolation, bidirectional power transfer, soft-switching capability, high power density, and excellent conversion efficiency [12], [13]. The incorporation of a High-Frequency Transformer (HFT) further improves electrical isolation while significantly reducing converter size and weight compared with conventional low-frequency transformer-based systems [14]. Consequently, DAB converters have become a preferred choice for high-power EV charging applications. Power transfer in the DAB converter is commonly controlled using Phase-Shifted Pulse Width Modulation (PSPWM), where the phase difference between the primary and secondary bridges regulates the transferred power [15]. This control strategy provides smooth bidirectional energy flow, low switching losses, and rapid transient response, making it highly suitable for renewable energy integrated EV charging systems [16]. Conventional Proportional–Integral (PI) controllers are widely used for converter control because of their simple implementation and ease of design [17]. However, PI controllers often exhibit degraded performance under nonlinear operating conditions caused by renewable energy intermittency, battery dynamics, and sudden load variations [18]. Their fixed controller parameters may lead to slower transient response, increased overshoot, and steady-state errors during dynamic operating conditions. To overcome these limitations, Artificial Neural Network (ANN)-based control techniques have attracted significant attention in renewable energy and power electronic applications. ANN controllers possess excellent nonlinear mapping capability, adaptive learning characteristics, and robust control performance without requiring an accurate mathematical model of the system [19], [20]. In the proposed work, an ANN-based current controller generates the phase-shift command for the PSPWM-controlled DAB converter, enabling accurate charging current regulation, improved dynamic response, and efficient bidirectional power transfer between the DC-link and the EV battery [21]. The complete renewable energy integrated EV charging system consists of a Solar PV array with P&O MPPT-controlled boost converter, a Battery Energy Storage System interfaced through a bidirectional buck–boost converter with voltage and current control, and an isolated Dual Active Bridge converter controlled by an ANN-based current controller. The proposed system is developed and simulated in the MATLAB/Simulink environment to evaluate its performance under different operating conditions. Simulation results demonstrate stable DC-link voltage regulation, effective power sharing between the Solar PV source and BESS, reduced current ripple, improved EV battery state of charge (SOC), and enhanced charging efficiency [22], [23]. The proposed charging architecture provides a reliable, intelligent, and energy-efficient solution for next-generation renewable energy-powered EV charging infrastructure and supports the development of sustainable smart grid technologies [24].

The main contributions of this work are summarized as follows:

1. Development of a renewable energy integrated bidirectional EV charging system using Solar PV and Battery Energy Storage System.
2. Implementation of a P&O MPPT-controlled DC–DC boost converter for maximum solar energy extraction.
3. Design of a bidirectional buck–boost converter with voltage and current control for efficient battery energy management.
4. Integration of an isolated Dual Active Bridge converter employing Phase-Shifted PWM for high-efficiency bidirectional power transfer.
5. Development of an ANN-based current controller to improve charging current regulation, dynamic response, and overall converter performance.

II. SYSTEM CONFIGURATION

Fig. 1 illustrates the configuration of the proposed ANN-based renewable energy integrated bidirectional EV charging system. The system consists of a Solar Photovoltaic (PV) array, a DC–DC boost converter, a Battery Energy Storage System (BESS) with a bidirectional buck–boost converter, a common DC-link, an isolated Dual Active Bridge (DAB) converter with a High-Frequency Transformer (HFT), and an EV battery. The Solar PV system employs a Perturb and Observe (P&O) MPPT algorithm to extract maximum power, while the boost converter regulates the PV output voltage. The BESS is connected through a bidirectional buck–boost converter with voltage and current control to manage battery charging and discharging while maintaining DC-link stability. The DAB converter transfers power between the DC-link and the EV battery using Phase-Shifted Pulse Width Modulation (PSPWM) controlled by an Artificial Neural Network (ANN)-based current controller. The proposed configuration enables efficient bidirectional power flow, stable DC-link voltage, improved charging performance, and reliable operation under varying renewable energy and load conditions.

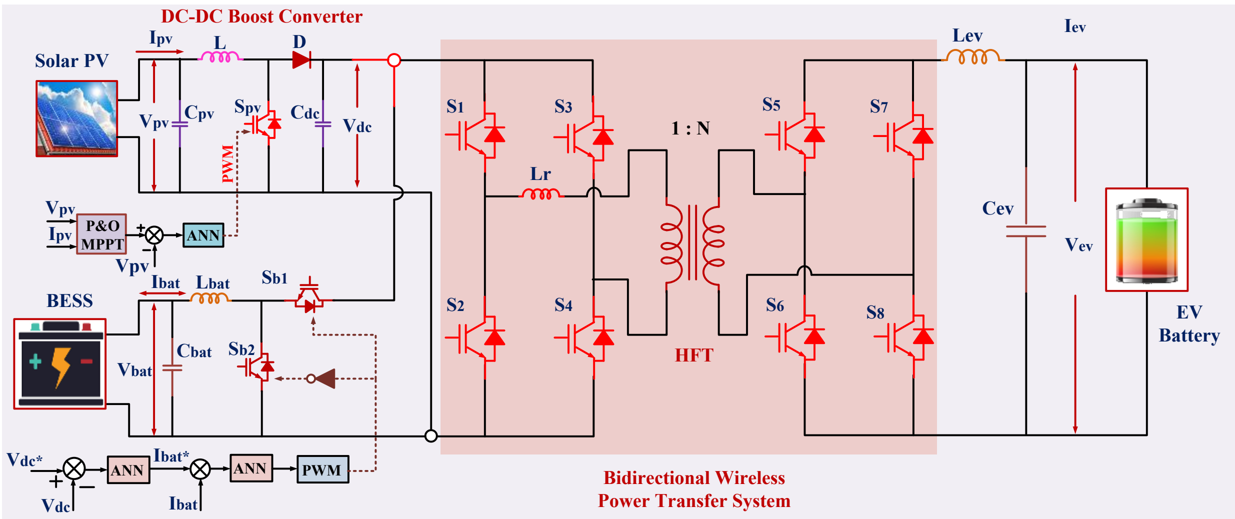

Fig. 1. Configuration of the Proposed Solar PV and BESS Based EV Charging System

III. SOLAR PV MODEL

A. Equivalent Circuit of the Single-Diode Solar PV Model

The single-diode model is one of the most used mathematical models for photovoltaic (PV) cell electrical activity because it balances modeling accuracy and computing simplicity. It properly describes the nonlinear current–voltage I–V properties of a solar cell under different environmental circumstances and is widely utilized in power system simulations and MPPT. The single-diode PV model's corresponding circuit includes a photocurrent source Iph, a diode D in parallel with it, a series resistance Rs, and a shunt resistance Rsh as shown in Fig. 2. The diode models the photovoltaic cell's p–n junction, while the photocurrent source represents incident solar irradiation. Series resistance accounts for semiconductor, metallic, and connector internal losses. Shunt resistance represents manufacturing and junction flaw leakage currents. The PV cell's output current is the difference between the photocurrent and the diode and shunt resistance currents. The analogous circuit accurately predicts PV module electrical performance under varying irradiance and temperature circumstances and is used to construct MPPT controllers.

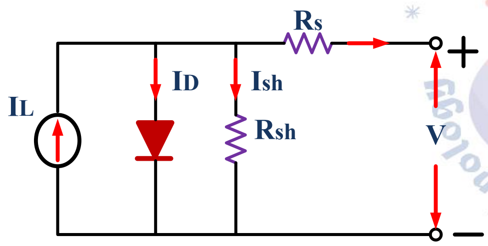

Fig. 2. Equivalent Circuit of the Single-Diode Solar PV Model

B. Mathematical Model

The output current of the single-diode PV model is expressed as

$$I = I_{Ph} - I_D - I_{sh} \tag{1}$$

Where

$$I_D = I_0\left[\exp\left(\frac{V+IR_s}{aV_t}\right) - 1\right] \tag{2}$$

And

$$I_{sh} = \frac{V+IR_s}{R_{sh}} \tag{3}$$

Therefore, the complete PV current equation becomes

$$I = I_{Ph} - I_0\left[\exp\left(\frac{V+IR_s}{aV_t}\right) - 1\right] - \frac{V+IR_s}{R_{sh}} \tag{4}$$

where

- I = Output current(A)
- V = Output voltage(V)
- I_{ph} = Photocurrent(A)
- I_0 = Reverse saturation current(A)
- R_s = Series resistance(Ω)
- R_{sh} = Shunt resistance(Ω)
- a = Diode ideality factor
- V_t = Thermal voltage(V)

The thermal voltage is given by

$$V_t = \frac{N_s kT}{q} \tag{5}$$

where

- N_S = Number of series connected cells
- $k = 1.381 * 10^{-23}$ J/K (Boltzmann constant)
- T = Cell temperature (K)
- $q = 1.602 * 10^{-19}$ C (Electron charge)

The photocurrent is calculated as

$$I_{Ph} = [I_{sc} + K_i(T - T_{ref})]\frac{G}{G_{ref}} \tag{6}$$

where

- I_{sc} = Short circuit current(A)
- K_i = Tempreature coefficient of current(A/C)
- G = Solar irradiance(W/m^2)
- G_{ref} = 1000 W / m^2
- $T_{ref} = 25^0$C

IV. PERTURB AND OBSERVE (P&O) MAXIMUM POWER POINT TRACKING (MPPT) ALGORITHM

The Perturb and Observe (P&O) algorithm is a widely used Maximum Power Point Tracking (MPPT) technique due to its simple implementation and effective tracking performance. In the proposed system, the P&O algorithm continuously measures the PV voltage VPV and PV current IPV to calculate the output power of the photovoltaic array. The operating point is periodically perturbed by adjusting the duty cycle of the DC–DC boost converter, and the corresponding change in PV power is observed. If the output power increases, the perturbation continues in the same direction; otherwise, the direction is reversed. This process enables the PV system to operate near the Maximum Power Point (MPP) under varying solar irradiance and temperature conditions as shown in Fig.1. The regulated output of the boost converter maintains a stable DC-link voltage and supplies maximum available solar power to the Battery Energy Storage System (BESS) and the Dual Active Bridge (DAB) converter for efficient EV battery charging. The PV output power is calculated as

$$P_{PV} = V_{PV} \times I_{PV} \tag{7}$$

Where

- P_{PV} = PV output power (W)
- V_{PV} = PV output voltage (V)

- I_{PV} = PV output current (A)

The operating principle of the P&O algorithm is summarized as follows:

1. Measure the PV voltage VPV and current IPV.
2. Calculate the instantaneous PV power:

$$P(k) = V(k) \times I(k) \tag{8}$$

3. Compare the present power P(k) with the previous power P(k−1).
4. If P(k)>P(k−1), continue perturbing the duty cycle in the same direction.
5. If P(k)<P(k−1), reverse the perturbation direction.
6. Repeat the process continuously until the operating point oscillates around the Maximum Power Point (MPP).

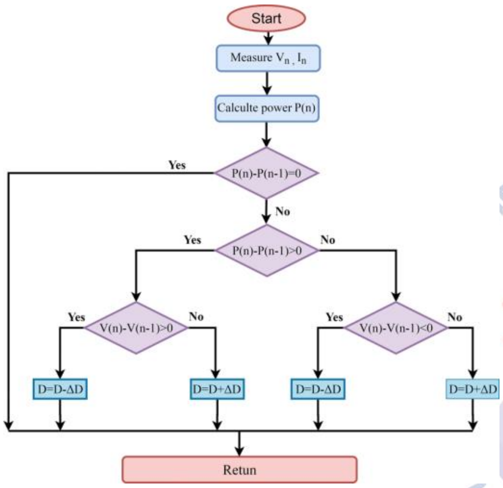

Fig.3 flow chart for P&O MPPT algorithm

V. WORKING OPERATION OF THE BIDIRECTIONAL BUCK–BOOST CONVERTER FOR THE BATTERY ENERGY STORAGE SYSTEM (BESS)

The Battery Energy Storage System (BESS) is connected to the common DC-link through a bidirectional buck–boost converter, enabling bidirectional energy flow between the battery and the DC-link as shown in Fig.5. The converter operates in buck mode during battery charging and boost mode during battery discharging. An Artificial Neural Network (ANN)-based voltage and current controller is employed to regulate the converter operation and maintain a stable DC-link voltage under varying renewable energy generation and EV charging conditions as shown in Fig.1.

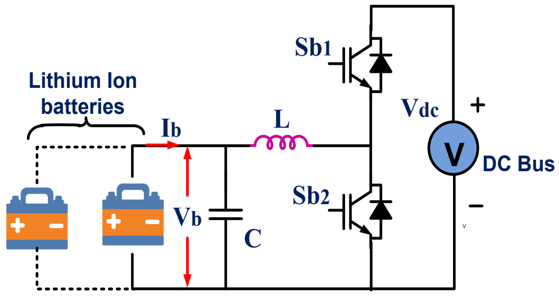

Fig.4 principle operation bidirectional dc-dc buck boost converter

The ANN controller continuously measures the DC-link voltage V_{dc}, battery voltage V_{bat}, and battery current II_{bat}. The measured DC-link voltage is compared with the reference voltage to generate the voltage error

$$e_v = V_{dc}^* - V_{dc} \tag{9}$$

Similarly, the battery current error is calculated as

$$e_i = I_{bat}^* - I_{bat} \tag{10}$$

The voltage error, current error, and their previous values are supplied as inputs to the ANN controller. The ANN processes these signals through its hidden layer neurons and produces the optimal duty cycle D for the bidirectional buck–boost converter.

The ANN output is expressed as

$$D = f_{ANN}(e_v, e_i) \tag{11}$$

where

- D = Converter duty cycle
- f_{ANN} = Nonlinear mapping function of the Artificial Neural Network

1. Battery Charging (Buck Mode)

When the Solar PV system generates excess power, the converter operates in buck mode, transferring energy from the DC-link to the battery. The battery charging voltage is

$$V_{bat} = DV_{dc}$$

The battery charging power is

$$P_{bat} = V_{bat} I_{bat}$$

2. Battery Discharging (Boost Mode)

When the Solar PV power is insufficient to meet the EV charging demand, the converter operates in **boost mode**, supplying energy from the battery to the DC-link. The output voltage is

$$V_{dc} = \frac{V_{bat}}{1-D} \tag{12}$$

The power delivered to the DC-link is

$$P_{dc} = V_{dc} I_{dc}$$

The battery State of Charge (SOC) is calculated as

$$SOC(t) = SOC(0) - \frac{1}{Q_{bat}} \int I_{bat} \, dt \tag{13}$$

where

- $SOC(0)$ = Initial battery state of charge
- Q_{bat} = Battery capacity (Ah)
- I_{bat} = Battery current (A)

The ANN controller continuously updates the converter duty cycle according to changes in the DC-link voltage, battery current, and system operating conditions. This intelligent control strategy enables smooth transitions between charging and discharging modes, minimizes voltage fluctuations, improves current regulation, enhances battery utilization, and maintains stable power flow to the Dual Active Bridge (DAB) converter. Consequently, the proposed ANN-controlled bidirectional buck–boost converter improves overall system efficiency and ensures reliable operation of the renewable energy integrated EV charging system.

VI. DUAL ACTIVE BRIDGE (DAB) CONVERTER: DESIGN, WORKING OPERATION, AND STATE-SPACE MODEL

A. Working Operation of the Dual Active Bridge (DAB) Converter

The Dual Active Bridge (DAB) converter is an isolated bidirectional DC–DC converter widely employed in electric vehicle (EV) charging applications due to its high efficiency, galvanic isolation, bidirectional power flow capability, and soft-switching operation. As shown in Fig. 5, the converter consists of two full-bridge converters interconnected through a High-Frequency Transformer (HFT) and a series leakage inductance Lr. The primary bridge is connected to the DC-link supplied by the Solar PV system and Battery Energy Storage System (BESS), whereas the secondary bridge is connected to the EV battery. In the proposed system, Phase-Shifted Pulse Width Modulation (PSPWM) is used to control the DAB converter. Both full bridges generate 50% duty-cycle square-wave voltages. The transferred power is controlled by varying the phase-shift angle ϕ between the primary and secondary bridge voltages. When the primary bridge voltage leads the secondary bridge voltage, power flows from the renewable energy source to the EV battery (Grid-to-Vehicle, G2V). Conversely, when the secondary bridge voltage leads the primary bridge voltage, power flows from the EV battery to the DC-link (Vehicle-to-Grid, V2G). The leakage inductance of the transformer stores and transfers energy between the two bridges while limiting the circulating current. The high-frequency transformer provides galvanic isolation, improves safety, and reduces the size and weight of the converter. The proposed ANN-based current controller continuously regulates the phase-shift angle according to the charging current demand, thereby ensuring accurate power regulation, reduced current ripple, and improved dynamic response.

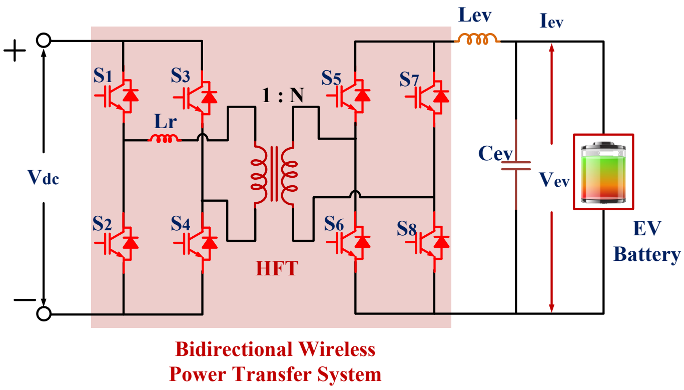

Fig. 5. Proposed ANN-Controlled Dual Active Bridge Converter for Bidirectional EV Charging

B. Design Equations

1. Transformer Turns Ratio

The transformer turns ratio is

$$n = \frac{N_s}{N_P} \quad (14)$$

where

- Np = Primary winding turns
- Ns = Secondary winding turns
- n = Transformer turns ratio

The transformer turns ratio determines the voltage conversion between the primary and secondary bridges. It is selected according to the required EV battery voltage.

2. Primary Bridge Voltage

The primary bridge generates a square-wave voltage

$$V_p = \pm V_{dc} \quad (15)$$

where

- V_{dc} = DC-link voltage

The primary full bridge converts the DC-link voltage into a high-frequency AC square wave.

3. Secondary Bridge Voltage

The secondary bridge voltage is

$$V_s = \pm \frac{V_{ev}}{n} \quad (16)$$

where

- V_{ev} = EV battery voltage

The secondary bridge converts the transformer output into DC for charging the EV battery.

4. Leakage Inductor Voltage

Applying Kirchhoff's Voltage Law,

$$V_L = V_p - \frac{V_s}{n} \quad (17)$$

The voltage across the leakage inductance is equal to the difference between the primary and reflected secondary voltages.

5. Inductor Current

The inductor current is governed by

$$L_r \frac{di_L}{dt} = V_p - \frac{V_s}{n} \quad (18)$$

where

- L_r = Leakage inductance
- i_L = Inductor current

This equation describes the rate of change of current flowing through the transformer leakage inductance. The current increases when the primary voltage is greater than the reflected secondary voltage and decreases otherwise.

6. Power Transfer Equation

The transferred power is

$$P = \frac{nV_{dc}V_{ev}}{\omega L_r} \phi \left(1 - \frac{\phi}{\pi}\right) \quad (19)$$

Where

- P = Output power
- $\omega = 2\pi fs$
- fs = Switching frequency
- ϕ = Phase-shift angle

The transferred power depends on

- DC-link voltage
- EV battery voltage
- Leakage inductance
- Switching frequency
- Phase-shift angle

Increasing the phase shift increases the transferred power.

Small Signal Approximation

For

$\emptyset < 30°$

the equation becomes

$$P = \frac{nV_{dc}V_{ev}}{\omega L_r} \phi \quad (20)$$

This simplified equation is commonly used for controller design because power is approximately proportional to the phase-shift angle.

7. Output Power

The output power delivered to the EV battery is

$$P_o = V_{ev} I_{ev} \quad (21)$$

where

- Iev = Battery charging current

8. Converter Efficiency

$$\eta = \frac{P_o}{P_{in}} \times 100\% \quad (22)$$

Where

- Po = Output power
- Pin = Input power

This equation represents the efficiency of the DAB converter.

VII. ANN-BASED CURRENT CONTROLLER DESIGN FOR THE DUAL ACTIVE BRIDGE CONVERTER

The proposed Dual Active Bridge (DAB) converter employs an Artificial Neural Network (ANN)-based current controller to regulate the EV battery charging current as shown in Fig.6. The controller generates the optimal duty ratio (or phase-shift command) for the Phase-Shifted Pulse Width Modulation (PSPWM) block, which produces the switching signals for the primary and secondary full-bridge switches S1–S8. The measured battery current is continuously compared with the reference charging current to generate the current error. The ANN controller processes the error and produces the control signal required for the DAB converter.

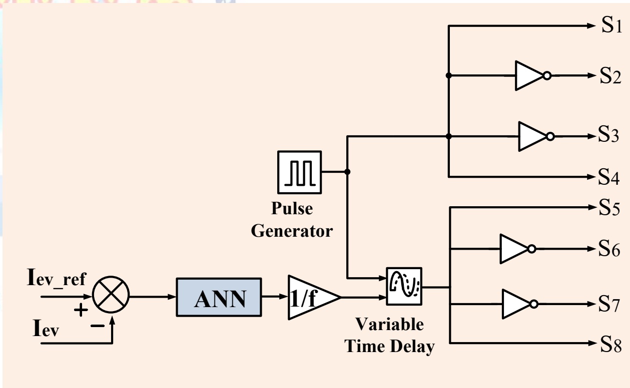

Fig. 6. ANN-Based Current Controller for the Dual Active Bridge (DAB) Converter

Current Error

The battery current error is

$$e(k) = I_b^*(k) - I_b(k) \quad (23)$$

where

- I_b^* = Reference battery current (A)
- I_b = Measured battery current (A)

Change in Current Error

The change in error is

$$\Delta e(k) = e(k) - e(k-1) \quad (24)$$

Where e(k) = Present error, e(k−1) = Previous error

ANN Input Vector

The ANN receives two input signals

$$X = \begin{bmatrix} e(k) \\ \Delta e(k) \end{bmatrix} \quad (25)$$

Where $e(k)$ = Current error, $\Delta e(k)$ = Change in current error

Hidden Layer Output

Each hidden neuron computes

$$h_j = f\left(\sum_{i=1}^{n} w_{ij} x_i + b_j\right) \quad (26)$$

where

- w_{ij}= Weight between input and hidden layer
- x_i = Input signal
- b_j = Hidden layer bias
- f(·) = Activation function

The sigmoid activation function is

$$f(x) = \frac{1}{1+e^{-x}} \quad (27)$$

Output Layer

The ANN output is

$$u = \sum_{j=1}^{m} v_j h_j + b_o \quad (28)$$

where

- u = ANN controller output
- v_j = Output layer weight
- b_o = Output layer bias

Duty Ratio (Phase-Shift Command)

The ANN output is converted into the duty ratio (or phase-shift angle)

$$\phi = u \quad (29)$$

where

- D = PWM duty ratio
- ϕ = Phase-shift angle

PWM Generation

The PWM pulse is generated as

$$PWM = \begin{cases} 1, V_C > V_{tri} \\ 0, V_C < V_{tri} \end{cases} \quad (30)$$

where

- V_C = ANN controller output
- V_{tri} = Carrier triangular waveform

The PWM block generates eight switching pulses

$s_1, s_2, s_3, s_4, s_5, s_6, s_7, s_8$

for the DAB converter.

VIII. SIMULATION RESULTS AND DISCUSSION

The proposed ANN-based renewable energy integrated bidirectional EV charging system was developed and simulated in the MATLAB/Simulink environment to evaluate its dynamic and steady-state performance. The system consists of a Solar PV array with a P&O MPPT-controlled DC–DC boost converter, a Battery Energy Storage System (BESS) connected through an ANN-controlled bidirectional buck–boost converter, and an isolated Dual Active Bridge (DAB) converter employing an ANN-based current controller with Phase-Shifted PWM (PSPWM). The simulation investigates the PV characteristics, DC-link voltage regulation, BESS performance, EV battery charging characteristics, and the comparative performance of the proposed ANN controller with the conventional PI controller.

A. Solar PV Performance

Fig. 7 illustrates the output voltage, current, and power characteristics of the Solar PV system under varying operating conditions. During the initial startup, the PV voltage rapidly increases and stabilizes at approximately 300 V, indicating effective voltage regulation by the DC–DC boost converter. Simultaneously, the PV current initially reaches about 35 A and gradually decreases with variations in solar irradiance and load demand. Consequently, the PV output power changes from approximately 10.5 kW to 7.8 kW and finally to 3.2 kW, corresponding to the available solar energy. Despite these variations, the Perturb and Observe (P&O) MPPT algorithm continuously tracks the maximum power point by adjusting the converter duty cycle, ensuring efficient maximum power extraction, stable converter operation, and reliable power delivery to the DC-link.

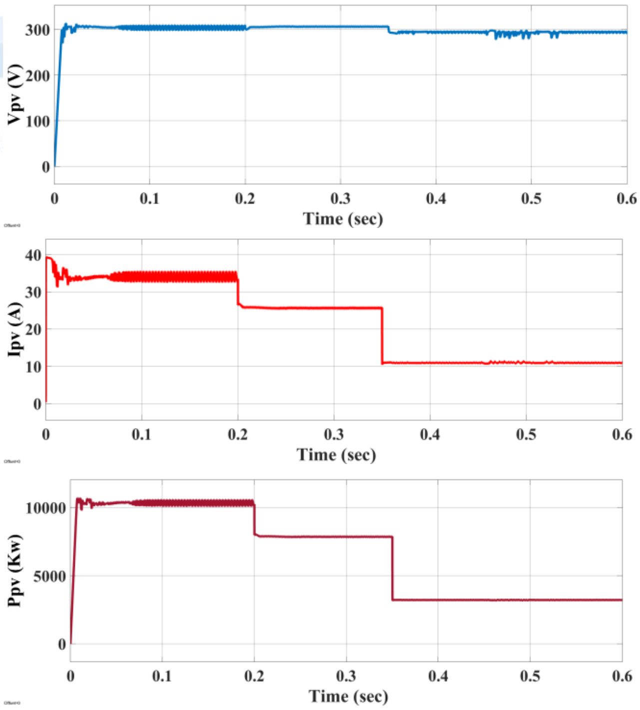

Fig. 7. Performance Characteristics of the Solar Photovoltaic (PV) System

B. DC-Link Voltage Regulation

Fig. 8 compares the DC-link voltage responses obtained using the conventional PI controller and the proposed ANN controller. Both controllers regulate the DC-link voltage around the reference value of 400 V. However, the PI controller exhibits a considerable overshoot during startup and a significant voltage dip during load disturbances. In contrast, the ANN controller provides a much smoother transient response with negligible overshoot, faster settling time, and improved voltage regulation. The results confirm that the ANN controller enhances DC-link stability and improves the overall dynamic performance of the charging system.

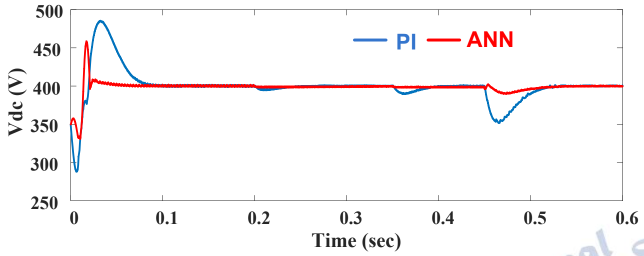

Fig. 8. Comparison of DC-Link Voltage Response under PI and ANN Controllers

C. Battery Energy Storage System (BESS) Performance

Fig. 9 illustrates the voltage, current, and State of Charge (SOC) characteristics of the Battery Energy Storage System (BESS). The BESS terminal voltage remains nearly constant at approximately 320 V, demonstrating effective voltage regulation by the ANN-controlled bidirectional buck–boost converter during both charging and discharging operations. Initially, the battery operates in charging mode, indicated by a negative current, where excess energy generated by the Solar PV system is stored in the battery. As the load demand increases and the available PV power decreases, the converter smoothly transitions to discharging mode, resulting in a positive battery current that supports the DC-link voltage. Consequently, the BESS SOC gradually increases during the charging period and slightly decreases during discharging, confirming efficient bidirectional energy management, smooth mode transition, and effective utilization of the battery energy storage system.

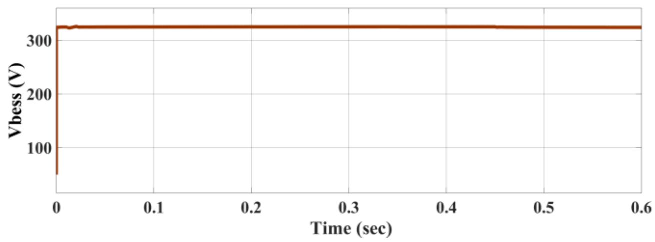

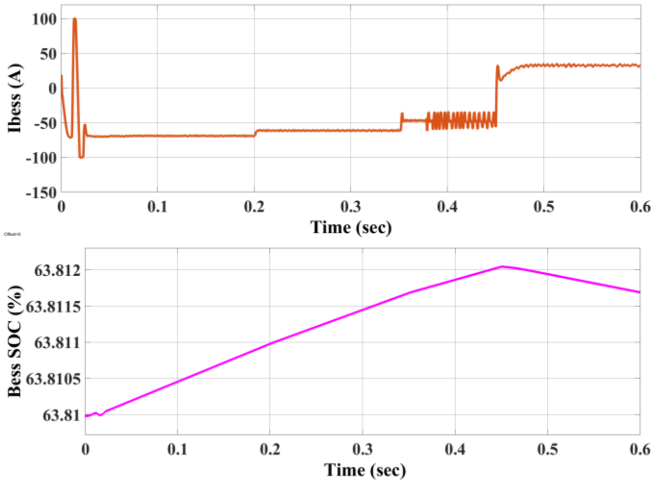

Fig. 9. Voltage, Current, and State of Charge (SOC) Characteristics of the Battery Energy Storage System (BESS)

D. EV Battery Charging Performance

Fig. 10 presents the voltage, charging current, and State of Charge (SOC) characteristics of the EV battery under both PI and ANN control strategies. The proposed ANN controller achieves faster voltage regulation with reduced overshoot and improved steady-state accuracy, maintaining the battery voltage close to its reference value throughout the charging process. The EV charging current accurately follows the reference current during charging and smoothly transitions during bidirectional power transfer, exhibiting superior current tracking, faster transient response, and reduced oscillations compared with the conventional PI controller. Furthermore, the EV battery SOC increases smoothly during charging and decreases gradually during discharging, indicating effective battery energy management. The improved SOC profile obtained with the ANN controller confirms enhanced charging efficiency, stable converter operation, and reliable bidirectional power transfer for the proposed EV charging system.

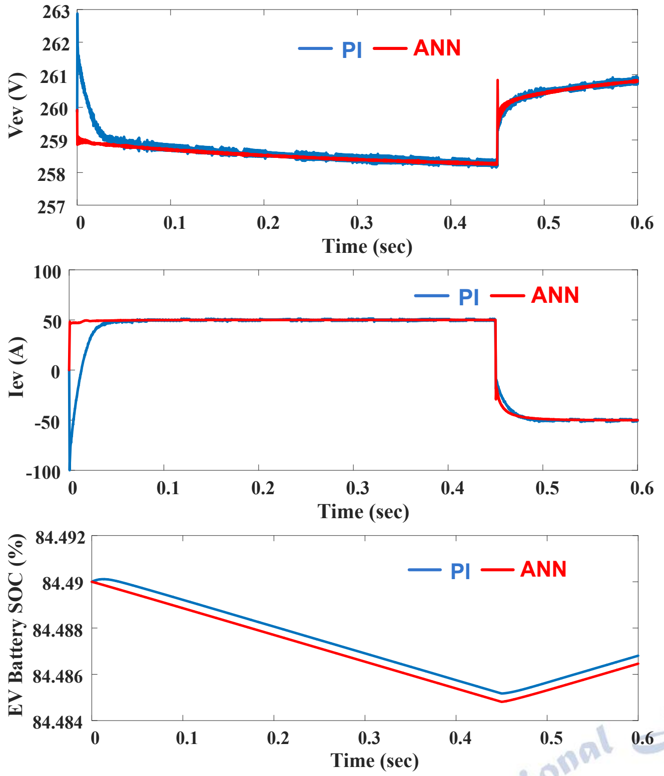

Fig. 10. Voltage, Current, and State of Charge (SOC) Characteristics of the EV Battery

E. DAB Converter Performance

Fig. 11 illustrates the primary voltage, primary current, secondary voltage, and secondary current waveforms of the proposed Dual Active Bridge (DAB) converter operating under the ANN-based Phase-Shifted Pulse Width Modulation (PSPWM) control strategy. The primary bridge generates a high-frequency square-wave voltage with an amplitude of approximately ±400 V, while the corresponding primary current remains stable with only minor transient variations, indicating efficient power transfer. Similarly, the secondary bridge produces a regulated square-wave voltage of approximately ±130 V, and the secondary current follows a smooth high-frequency waveform with minimal oscillations during steady-state operation. The enlarged waveforms confirm the generation of complementary gate pulses and proper phase-shift operation between the primary and secondary bridges. The results demonstrate that the proposed ANN-controlled DAB converter achieves stable bidirectional power transfer, reduced current ripple, effective transformer utilization, and high conversion efficiency, thereby ensuring reliable charging and discharging operation of the EV battery.

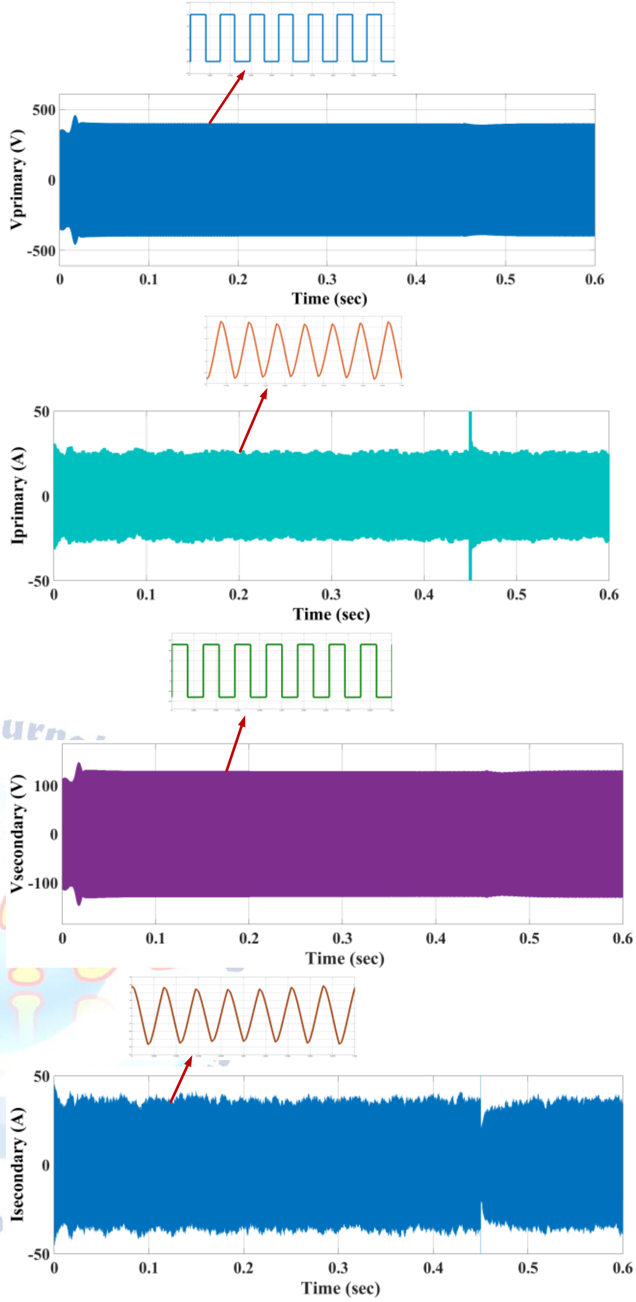

Fig. 11. Primary and Secondary Voltage and Current Characteristics of the Proposed Dual Active Bridge (DAB) Converter.

IX CONCLUSION

This paper presented an ANN-based renewable energy integrated bidirectional EV charging system using a Solar PV source, Battery Energy Storage System (BESS), DC–DC boost converter, bidirectional buck–boost converter, and an isolated Dual Active Bridge (DAB) converter. The Solar PV system employed the P&O MPPT algorithm to maximize power extraction, while the ANN-based voltage, current, and DAB current controllers ensured stable DC-link voltage, efficient battery energy management, and reliable bidirectional power transfer. Simulation results obtained in MATLAB/Simulink demonstrated improved PV power extraction, stable BESS operation, enhanced EV battery charging performance, and superior dynamic response compared with the conventional PI controller. The proposed ANN-based control strategy provides an efficient, reliable, and intelligent solution for renewable energy-powered bidirectional EV charging applications.

Conflict of interest statement

Authors declare that they do not have any conflict of interest.

REFERENCES

[1] M. Yilmaz and P. T. Krein, "Review of battery charger topologies, charging power levels, and infrastructure for plug-in electric and hybrid vehicles," IEEE Transactions on Power Electronics, vol. 28, no. 5, pp. 2151–2169, 2013.

[2] S. Habib, M. Kamran, and U. Rashid, "Impact analysis of vehicle-to-grid technology and charging strategies of electric vehicles on distribution networks," Journal of Power Sources, vol. 277, pp. 205–214, 2015.

[3] T. Esram and P. L. Chapman, "Comparison of photovoltaic array maximum power point tracking techniques," IEEE Transactions on Energy Conversion, vol. 22, no. 2, pp. 439–449, 2007.

[4] N. Femia, G. Petrone, G. Spagnuolo, and M. Vitelli, "Optimization of perturb and observe maximum power point tracking method," IEEE Transactions on Power Electronics, vol. 20, no. 4, pp. 963–973, 2005.

[5] V. Salas, E. Olias, A. Barrado, and A. Lazaro, "Review of the maximum power point tracking algorithms for stand-alone photovoltaic systems," Solar Energy Materials and Solar Cells, vol. 90, pp. 1555–1578, 2006.

[6] F. Blaabjerg, Y. Yang, D. Yang, and X. Wang, "Distributed power-generation systems and protection," Proceedings of the IEEE, vol. 105, no. 7, pp. 1311–1331, 2017.

[7] A. Khaligh and O. C. Onar, Energy Harvesting: Solar, Wind and Ocean Energy Conversion Systems. CRC Press, 2010.

[8] H. Ibrahim, A. Ilinca, and J. Perron, "Energy storage systems characteristics and comparisons," Renewable and Sustainable Energy Reviews, vol. 12, pp. 1221–1250, 2008.

[9] R. W. De Doncker, D. M. Divan, and M. H. Kheraluwala, "A three-phase soft-switched high-power-density DC/DC converter for high-power applications," IEEE Transactions on Industry Applications, vol. 27, no. 1, pp. 63–73, 1991.

[10] H. Bai and C. Mi, "Eliminate reactive power and increase system efficiency of isolated bidirectional dual-active-bridge DC–DC converters using novel dual-phase-shift control," IEEE Transactions on Power Electronics, vol. 23, no. 6, pp. 2905–2914, 2008.

[11] F. Krismer and J. W. Kolar, "Efficiency-optimized high-current dual active bridge converter," IEEE Transactions on Industrial Electronics, vol. 59, no. 7, pp. 2745–2760, 2012.

[12] G. Guidi, M. Pavlovsky, A. Kawamura, T. Imakubo, and Y. Sasaki, "Improvement of light load efficiency of dual active bridge DC–DC converter by using dual phase shift control," IEEE Transactions on Power Electronics, vol. 28, no. 8, pp. 3786–3800, 2013.

[13] X. Tang, C. Sun, S. Bi, S. Wang, and A. Zhang, "A holistic review on advanced bidirectional EV charging control algorithms," 2022.

[14] K. S. P. Oruganti et al., "An integrative review of standalone solar-powered EV charging stations," Energy Reports, 2025.

[15] H. Sarwar Khan, I. S. Mohamed, K. Kauhaniemi, and L. Liu, "Artificial Neural Network-Based Voltage Control of DC/DC Converter for DC Microgrid Applications," 2021.

[16] D. Kolech et al., "ANN based energy management of solar integrated bidirectional EV charging stations for light electric vehicles," Discover Environment, 2026.

[17] J. M. Carrasco et al., "Power-electronic systems for the grid integration of renewable energy sources: A survey," IEEE Transactions on Industrial Electronics, vol. 53, no. 4, pp. 1002–1016, 2006.

[18] H. Abu-Rub, M. Malinowski, and K. Al-Haddad, Power Electronics for Renewable Energy Systems, Transportation and Industrial Applications. Wiley, 2014.

[19] B. Singh, B. N. Singh, A. Chandra, K. Al-Haddad, A. Pandey, and D. P. Kothari, "A review of single-phase improved power quality AC–DC converters," IEEE Transactions on Industrial Electronics, vol. 50, no. 5, pp. 962–981, 2003.

[20] H. Cha, T. Vu, and J. Kim, "Design and control of proportional–integral controller based bidirectional DC–DC converters," IEEE Transactions on Industrial Electronics.

[21] J. Srinu Naick et al., "An Intelligent ANN-Controlled Grid-Connected Solar PV System with Improved Stability for Multi-Application Energy Management," 2026.

[22] M. H. Rashid, Power Electronics: Circuits, Devices, and Applications, 4th ed. Pearson, 2014.

[23] N. Mohan, T. M. Undeland, and W. P. Robbins, Power Electronics: Converters, Applications, and Design, 3rd ed. Wiley, 2003.

[24] R. Teodorescu, M. Liserre, and P. Rodríguez, Grid Converters for Photovoltaic and Wind Power Systems. Wiley, 2011.